Effect of an in-plane magnetic field on microwave-assisted magnetotransport in a two-dimensional electron system

Jesús Iñarrea[1,2] and Gloria Platero[2]
[1]*Escuela Politécnica Superior, Universidad Carlos III, Leganes, Madrid 28911, Spain*
[2]*Unidad Asociada al Instituto de Ciencia de Materiales, CSIC, Cantoblanco, Madrid 28049, Spain*
(Received 30 October 2008; published 20 November 2008)

In this work we present a theoretical approach to study the effect of an in-plane (parallel) magnetic field on the microwave-assisted transport properties of a two-dimensional electron system. Previous experimental evidences show that microwave-induced resistance oscillations and zero resistance states are differently affected depending on the experimental setup: two magnetic fields (two-axis magnet) or one tilted magnetic field. In the first case, experiments report a clear quenching of resistance oscillations and zero resistance states. In a tilted field, one obtains oscillations displacement and quenching but the latter is unbalanced and less intense. In our theoretical proposal we explain these results in terms of the microwave-driven harmonic motion performed by the electronic orbits and how this motion is increasingly damped by the in-plane field.

DOI: 10.1103/PhysRevB.78.193310 PACS number(s): 73.40.−c, 73.50.−h, 78.67.−n

In recent years, with the rise of nanotechnology, a lot of effort has been devoted to the study and research of physics of nanodevices from theoretical, experimental, and application perspectives. In particular the response of such systems to external, time-dependent, or stationary fields is receiving much attention from the scientific community.[1] Remarkable examples are the recently obtained microwave (MW)-induced resistance oscillations (MIROs) and zero resistance states (ZRSs) (Refs. 2–4) in two-dimensional (2D) electron system (2DES). These striking results have been the subject of intense current interest in the condensed-matter community. Thus, different experimental evidences are being published in a continuous basis challenging the available theoretical models.[5–11] Among all of those experimental outcomes we can cite, for instance, temperature dependence of MIRO,[2,3,5] absolute negative conductivity,[12–14] bichromatic MW excitation,[3,15] polarization immunity of magnetoresistance (ρ_{xx}),[16–18] and the effect of MW frequency on MIRO and ZRS.[19,20] An important set of results on MIRO that has not yet received special attention from theorists is the effect of an in-plane magnetic field ($B_\parallel$) (parallel to the 2DES and x-y plane) on the transport properties of these devices. In a two-axis magnet experiment, we have two magnetic fields: $B_\parallel$ and the magnetic field perpendicular ($B_\perp$) to the 2DES.[21] In a tilted magnetic-field (B_{tilted}) experiment, we only have one field, and in this case $B_\parallel$ is the parallel component of B_{tilted}.[22] In the first case[21] (Yang's experiment) results show a strong suppression of MIRO and ZRS. The second case[22] (Mani's experiment) demonstrates a displacement of MIRO at larger B_{tilted} and an unbalanced quenching. Therefore these unexpected results deserve to be considered by the different theoretical approaches serving as a crucial test for them.

In this Brief Report we present a theoretical model to address those results, and we try to reconcile them using a common physical mechanism. When a 2DES is illuminated with MW radiation, electronic orbits are forced to move back and forth, oscillating harmonically at the frequency of MW radiation and with an amplitude proportional to the MW electric field.[5,14] MIRO are proportional to the magnitude of this amplitude and any variation of it is finally reflected on MIRO. In their MW-driven orbit motion, electrons interact with the lattice ions being damped, producing acoustic phonons. According to our model, the presence of $B_\parallel$ imposes an extra harmonically oscillating motion in the z direction enlarging the electrons trajectory in their orbits. This would increase the interactions with the lattice making the damping process more intense and reducing the amplitude of the orbit oscillations. However depending on the origin of $B_\parallel$, the damping intensity would be different. Thus, in Yang's experiment[21] the magnetic fields $B_\parallel$ and $B_\perp$ are not related, and $B_\parallel$ is kept constant while $B_\perp$ increases from zero. Thus, the effect of $B_\parallel$ is the same in the whole ρ_{xx} response, and MIROs are uniformly quenched. However in Mani's experiment $B_\parallel$ would not be constant because it depends on B_{tilted}. Then the quenching of MIRO would be unbalanced and only visible at larger values of B_{tilted}.

The Hamiltonian for electrons confined in a 2D system (x-y plane) by a potential $V(z)$ and subjected to a magnetic field $B=(B_x,0,B_z)$ ($B_\parallel=B_x$ and $B_\perp=B_z$) is given by

$$\begin{aligned} H_0 &= \frac{P_x^2+P_y^2}{2m^*}+\frac{w_z}{2}L_z+\frac{1}{2}m^*\left[\frac{w_z}{2}\right]^2(x^2+y^2)+\frac{P_z^2}{2m^*} \\ &\quad +\frac{1}{2}m^*w_x^2z^2+V(z)+\frac{1}{2}w_xz(exB_z-2P_y) \\ &= H_{xy}+H_z+\frac{1}{2}w_xz(exB_z-2P_y). \end{aligned} \tag{1}$$

We have used the symmetric gauge for B_z, $\overrightarrow{A_{B_z}}=-\frac{1}{2}\vec{r}\times\vec{B}=(-\frac{y}{2}B_z,\frac{x}{2}B_z,0)$, and the Landau gauge for B_x, $\overrightarrow{A_{B_x}}=(0,-zB_x,0)$. w_z is the cyclotron frequency of B_z, $w_z=\frac{eB_z}{m^*}$, and w_x is of B_x, $w_x=\frac{eB_x}{m^*}$. L_z is the z component of the electron total angular momentum. According to the experimental parameters used[21,22] the Hamiltonian term $\frac{1}{2}w_xz(exB_z-2P_y)\ll H_{xy}+H_z$. Then, we can discard this term and write $H_0\simeq H_{xy}+H_z$.

When one considers a parabolic potential for $V(z)$,

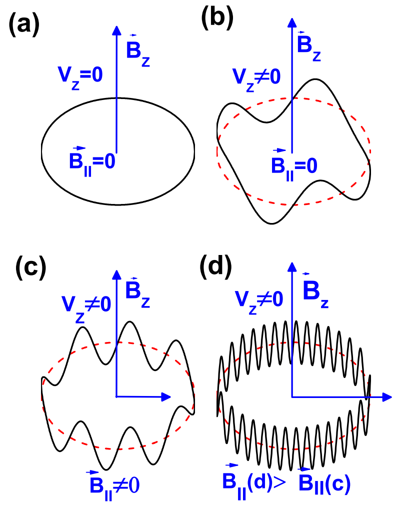

FIG. 1. (Color online) Schematics showing the semiclassical description of electron trajectories in 2D systems under different potentials and fields: (a) 2D (x-y plane) parabolic potential, (b) 2D+1D (z direction) parabolic potentials, and [(c) and (d)] 2D+1D parabolic potentials and an in-plane magnetic field $B_{\|}$.

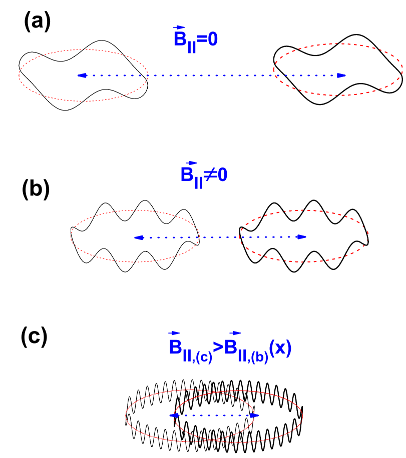

FIG. 2. (Color online) Schematic showing the dependence of MW-driven electronic orbit oscillating motion with $B_{\|}$. From (a) to (c), $B_{\|}$ intensity increases which makes the MW-driven amplitude smaller and smaller. Eventually the oscillating motion collapses, amplitude goes to zero, and MIROs are quenched.

$V(z)=\frac{1}{2}m^* w_0^2 z^2$, the Hamiltonian H_z can finally be written as

$$H_z = \frac{P_z^2}{2m^*} + \frac{1}{2}m^*(w_x^2 + w_0^2)z^2 = \frac{P_z^2}{2m^*} + \frac{1}{2}m^*\Omega^2 z^2 \qquad (2)$$

and the Schrödinger equation of H_0 can directly be solved. We obtain the wave functions of two harmonic oscillators, one is two dimensional in the x-y plane and the other one is one dimensional (1D) in the z direction. In a semiclassical approach the electron is subjected simultaneously to two independent harmonic motions with a trajectory depicted in Fig. 1: the electron performs a circular movement in the x-y plane and at the same time a 1D harmonic oscillating motion in the z direction. In Fig. 1(a) we present the semiclassical trajectory of an electron in a 2D parabolic potential: the electron trajectory is circular. In Fig. 1(b), we add a parabolic potential in the z direction, then the electron trajectory is circular in the plane and at the same time it is oscillating in z. In Figs. 1(c) and 1(d), we introduce $B_{\|}$ and the oscillations in z direction increase with the intensity of $B_{\|}$. We obtain similar results when $B_{\|}=B_y$.

The problem of two-dimensional electrons subjected to magnetic fields at arbitrary angles has been already solved analytically with a parabolic confinement in the perpendicular direction.[23,24] According to these results the Hamiltonian can be transformed through a rotation of the coordinate system with a certain angle. The obtained Hamiltonian corresponds to two Hamiltonians of quantum harmonic oscillators and can be exactly solved.[23,24]

If we now switch on the MW radiation (plane polarized in the x direction) and connect a constant electric field (E_{dc}) in the same direction (transport direction), the Hamiltonian then reads

$$H_T = \frac{P_x^2 + P_y^2}{2m^*} + \frac{w_z}{2}L_z + \frac{1}{2}m^*\left[\frac{w_z^2}{2}\right][(x-X)^2 + y^2] - \frac{1}{2}eE_{dc}X - eE_0(x-X)\cos wt - eE_0 X\cos wt + \frac{P_z^2}{2m^*} + \frac{1}{2}m^*\Omega^2 z^2. \qquad (3)$$

X is the center of the orbit for the electron spiral motion: $X=\frac{eE_{dc}}{m^*(w_c/2)^2}$. The corresponding time-dependent Schrödinger equation can be exactly solved,[5,14,15] and the wave functions are

$$\Psi_T(x,y,t) \propto \phi_N\{[x-X-a(t)],[y-b(t)],t\}\phi(z), \qquad (4)$$

where ϕ_N are Fock-Darwin states[25] and $\phi(z)$ is the one-dimensional harmonic-oscillator wave function. $a(t)$ (for the x coordinate) and $b(t)$ (for the y coordinate) are the solutions for a *classical* driven 2D harmonic oscillator. The expression, for instance, for $a(t)$ (Ref. 17) is $a(t)=\frac{eE_o}{m^*\sqrt{(w_z^2-w^2)^2+\gamma^4}}\cos wt = A\cos wt$, where E_0 is the amplitude of the MW electric field, w is the frequency, and e is the electron charge. γ is a damping factor which dramatically affects the movement of the MW-driven electronic orbits. Along with this movement interactions occur between electrons and lattice ions, yielding acoustic phonons and producing a damping effect in the electronic motion. In Refs. 5 and 20, we developed a microscopical model to calculate γ. We obtained that γ is a material and sample-dependent parameter which depends also on lattice temperature, electronic orbit length, and MW frequency.[5,20] As we have indicated above, in a semiclassical explanation the presence of $B_{\|}$ alters the electron trajectory in its orbit, increasing the frequency and the number of oscillations in the z direction (Fig. 2). Now the frequency of the z-oscillating motion is $\Omega > w_0$. This makes longer the electron trajectory increasing the total orbit length and eventually the damping. This increase in the orbit length is proportionally equivalent to the increase in the number of

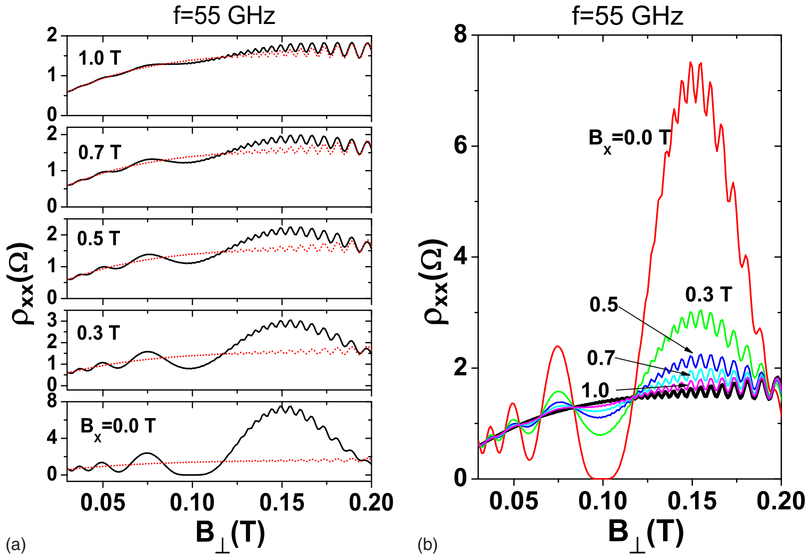

FIG. 3. (Color online) Calculated results of ρ_{xx} vs $B_\perp$ for different values of B_x from 0.0 to 1.0 T. $B_\perp$ and B_x are independent. In panel (a) we present the curves of each value of B_x in individual panels. Single lines correspond to MW on and dotted lines to MW off. We observe a progressive quenching of ρ_{xx} oscillations as B_x increases. In panel (b) we present all curves together for comparison. MW frequency is 55 GHz and $T=1$ K.

oscillations in the z direction. Thus, we introduce the ratio of frequencies after and before connecting $B_\parallel$ as a correction factor for the damping factor γ. The final damping parameter γ_f is

$$\gamma_f = \gamma \times \frac{\Omega}{w_0} = \gamma \times \sqrt{1 + \left(\frac{w_x}{w_0}\right)^2} = \gamma \times \sqrt{1 + \left(\frac{eB_x}{m^* w_0}\right)^2}. \quad (5)$$

Now, following a previous model developed by us,[5,14] we are able to calculate ρ_{xx}, whose result is proportional to the MW-induced oscillation amplitude of the electronic orbits center,

$$\rho_{xx} \propto A \cos w\tau = \frac{eE_o}{m^* \sqrt{(w_z^2 - w^2)^2 + \gamma_f^4}} \cos w\tau, \quad (6)$$

where τ is the charged impurity scattering time.[5,14] In Fig. 3 we present calculated results of ρ_{xx} vs $B_\perp$ for different values of B_x being independent of $B_\perp$ as in Yang's experiment. Thus, calculations have been made for a MW frequency of 55 GHz and a confinement in z of 50 nm (similar to Yang's experiment). B_x values are $B_x(T)=0.0$, 0.3, 0.5, 0.7, and 1.0. In the top panel we can see the results for each value of B_x in individual panels. We observe clearly the progressive quenching of MIRO as B_x increases. In the bottom panel we present all curves together in the same panel for comparison.

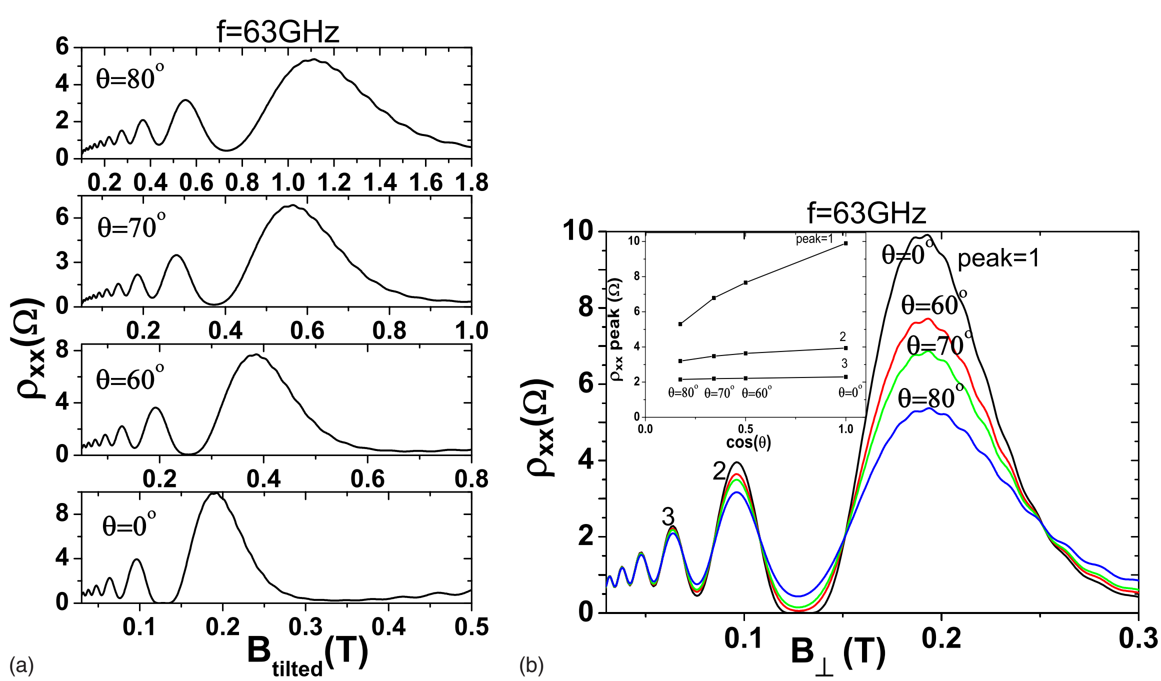

FIG. 4. (Color online) Calculated results of ρ_{xx} vs B_{tilted} for different values of θ. In panel (a) we present the curves of each value of θ in individual panels. In panel (b) we present all curves together for comparison to $B_\perp$. MW frequency is 63 GHz. In the inset we present the peak resistance vs cos θ and $T=1$ K.

According to Eqs. (5) and (6), when we increase B_x, we also increase the damping γ_f and as a result the amplitude A and MIRO are progressively quenched. We obtain a total quenching for $B_x \simeq 1.0$ T. We observe a uniform damping in the whole range of $B_\perp$ for each value of B_x. These results are in good agreement with experiment.[21] In Fig. 4 we present calculated results of ρ_{xx} vs B_{tilted} in the top panel and vs $B_\perp = B_{\text{tilted}} \cos\theta$ in the bottom panel. According to parameters and setup of Mani's experiment, we have used a confinement in z of 30 nm and MW frequency of 63 GHz. We present different curves corresponding to different tilt angles (θ). θ values are $\theta=0°$, 60°, 70°, and 80°. In this case $B_\parallel = B_{\text{tilted}} \sin\theta$. In the top panel we present calculated curves for each θ in individual panels. We observe MIRO displacement at larger B_{tilted} for increasing values of θ. This is explained considering that $B_\perp = B_{\text{tilted}} \cos\theta$ and that peak positions are only governed by $B_\perp$. In the bottom panel we can see all curves together for comparison. We observe, as in experiment, how the quenching effect is not uniform and more intense with increasing values of B_{tilted} and θ. Our model explains this peculiar behavior with the expression of $B_\parallel$ and Eqs. (5) and (6). Increasing values of B_{tilted} and θ give rise to an increasing damping according to Eq. (5) and decreasing A and MIRO according to Eq. (6). Thus, we observe a soft quenching for small values of $B_\perp$ and θ, and it gets progressively more important for larger values of them. This feature is shown in the inset of Fig. 4 in the bottom panel, where we present the peak resistance vs cos θ for peaks=1, 2, and 3, as in experiment.[22] The decrease in the peak resistance is larger for peak 1 than for peaks 2 and 3 as θ increases. These results are in good agreement with Mani's experiment.[22]

In summary, we have presented a theoretical model on the effect of an in-plane magnetic field on MIRO and ZRS in 2DES. Experimental results show different behaviors depending on the setup of the magnetic field. In an independent $B_\parallel$ experiments report a clear quenching of MIRO and ZRS. In a tilted B, experiments show oscillation displacement and an unbalanced quenching. We have presented a theoretical model which explains these results based on a common physical mechanism. The MW-driven oscillating electronic orbit motion is increasingly damped by the presence of $B_\parallel$. The understanding of this behavior will allow one to control the transport properties in a MW irradiated Hall bar, in particular, MIRO and ZRS features by tuning external magnetic fields in different configurations.

This work has been supported by the MCYT (Spain) under Grant No. MAT2005-0644 and by the Ramón y Cajal program.

[1] J. Iñarrea, G. Platero, and C. Tejedor, Semicond. Sci. Technol. **9**, 515 (1994); J. Iñarrea and G. Platero, Phys. Rev. B **51**, 5244 (1995); Europhys. Lett. **34**, 43 (1996).

[2] R. G. Mani, J. H. Smet, K. von Klitzing, V. Narayanamurti, W. B. Johnson, and V. Umansky, Nature (London) **420**, 646 (2002).

[3] M. A. Zudov, R. R. Du, L. N. Pfeiffer, and K. W. West, Phys. Rev. Lett. **90**, 046807 (2003).

[4] S. A. Studenikin, M. Potemski, A. Sachrajda, M. Hilke, L. N. Pfeiffer, and K. W. West, Phys. Rev. B **71**, 245313 (2005).

[5] J. Iñarrea and G. Platero, Phys. Rev. Lett. **94**, 016806 (2005); Phys. Rev. B **72**, 193414 (2005).

[6] A. C. Durst, S. Sachdev, N. Read, and S. M. Girvin, Phys. Rev. Lett. **91**, 086803 (2003).

[7] C. Joas, J. Dietel, and F. von Oppen, Phys. Rev. B **72**, 165323 (2005).

[8] X. L. Lei and S. Y. Liu, Phys. Rev. Lett. **91**, 226805 (2003); X. L. Lei, Appl. Phys. Lett. **90**, 132119 (2007).

[9] V. Ryzhii and V. Vyurkov, Phys. Rev. B **68**, 165406 (2003).

[10] P. H. Rivera and P. A. Schulz, Phys. Rev. B **70**, 075314 (2004).

[11] Manuel Torres and Alejandro Kunold, Phys. Rev. B **71**, 115313 (2005).

[12] R. L. Willett, L. N. Pfeiffer, and K. W. West, Phys. Rev. Lett. **93**, 026804 (2004).

[13] A. A. Bykov, D. R. Islamov, D. V. Nomokonov, and A. K. Bakarov, JETP Lett. **86**, 608 (2008).

[14] J. Iñarrea and G. Platero, Appl. Phys. Lett. **89**, 052109 (2006).

[15] J. Iñarrea and G. Platero, Appl. Phys. Lett. **89**, 172114 (2006).

[16] J. H. Smet, B. Gorshunov, C. Jiang, L. Pfeiffer, K. West, V. Umansky, M. Dressel, R. Meisels, F. Kuchar, and K. von Klitzing, Phys. Rev. Lett. **95**, 116804 (2005).

[17] J. Iñarrea and G. Platero, Phys. Rev. B **76**, 073311 (2007); J. Iñarrea, Appl. Phys. Lett. **90**, 172118 (2007); **90**, 262101 (2007).

[18] S. Wang and T.-K. Ng, Phys. Rev. B **77**, 165324 (2008).

[19] S. A. Studenikin, A. S. Sachrajda, J. A. Gupta, Z. R. Wasilewski, O. M. Fedorych, M. Byszewski, D. K. Maude, M. Potemski, M. Hilke, K. W. West, and L. N. Pfeiffer, Phys. Rev. B **76**, 165321 (2007).

[20] J. Iñarrea, Appl. Phys. Lett. **92**, 192113 (2008).

[21] C. L. Yang, R. R. Du, L. N. Pfeiffer, and K. W. West, Phys. Rev. B **74**, 045315 (2006).

[22] R. G. Mani, Phys. Rev. B **72**, 075327 (2005); Appl. Phys. Lett. **92**, 102107 (2008).

[23] J. C. Maan, *Two Dimensional Systems, Heterostructures and Superlattices* (Springer-Verlag, Berlin, 1984), p. 183.

[24] R. Merlin, Solid State Commun. **64**, 99 (1987).

[25] V. Fock, Z. Phys. **47**, 466 (1928); C. G. Darwin, Proc. Cambridge Philos. Soc. **27**, 86 (1930).